

BRUSHLESS DC MOTOR SYSTHESIS FOR ZERO TORQUE RIPPLE

Tahir Izhar¹ and P. D. Evans²

¹University of Engineering and Technology Lahore, Pakistan.

²University of Plymouth, U.K.

ABSTRACT

The use of permanent magnet brushless motors is increasing in many applications. These motors are highly attractive in servo applications. Smooth torque operation is one of the main requirements in such applications. This paper presents the synthesis of Brushless DC motor based on harmonic by harmonic method. A new approach to synthesize the magnetic design of the machine for zero torque ripple operation is addressed in this paper.

KEYWORDS

Permanent Magnet Brushless DC motor, torque ripple.

INTRODUCTION

Permanent Magnet Brushless (PMB) DC motors are highly attractive for servo applications due to their characteristics [1,2]. However, ripple-free torque operation is an essential requirement in these applications particularly at low speed. Since the frequencies of torque harmonics are above the frequencies to which the mechanical systems can respond, hence, torque ripple is usually filtered out at high speed by the system inertia. However, at low speed, torque ripple produces noticeable effects. Ideally a ripple-free torque operation can be achieved by constructing the motor so that it has either a sinusoidal or a trapezoidal back EMF. However, it is not always possible to produce desired induced EMFs and to feed the desired current with practical machine and drive design, hence torque pulsation is introduced. Ripple-free torque operation cannot be achieved with a quasi-square current because the induced EMF waveform is degraded due to non-ideal flux density distribution in the airgap. However, some authors have reported the use of modified current waveform to reduce the torque pulsation in PMB motors [3]-[7]. In this method, the phase current is programmed so that the torque pulsation, produced by non-ideal induced EMF, is cancelled. Selective current harmonic injection techniques have also been proposed [8]-[10] to minimize the torque pulsation. However, these techniques require high resolution rotor-position sensors and complicated controllers.

In this paper a new design method of magnetic circuit of Brushless DC motor is presented for ripple-free torque operation. Motor induced EMF is synthesized using harmonic-by-harmonic technique for zero torque pulsation. The airgap flux density distribution is synthesized for a few typical winding designs.

PRODUCTION OF ELECTROMAGNETIC TORQUE

The electromagnetic torque is produced by the interaction of induced EMF of the motor and the feed current [11]. Therefore, for a q-phase machine, the instantaneous torque can be expressed as

$$T_{em} = \frac{\pi p D L_{stk}}{2} \sum_{k=1}^q \sum_{n=1}^{\infty} \sum_{m=1}^{\infty} I_m B_n Z_n \cdot \begin{cases} \cos \left[n \left(\omega t - \frac{2\pi}{q} (k-1) \right) + n\gamma \right] \\ \cos \left[m \left(\omega t - \frac{2\pi}{q} (k-1) \right) \right] \end{cases} \quad (1)$$

which, manipulating the trigonometric identities, gives:

$$T_{em} = \frac{\pi p D L_{stk}}{4} \sum_{k=1}^q \sum_{n=1}^{\infty} \sum_{m=1}^{\infty} I_m B_n Z_n \cdot \begin{cases} \cos \left[(n+m) \left(\omega t - \frac{2\pi}{q} (k-1) \right) + n\gamma \right] + \\ \cos \left[(n-m) \left(\omega t - \frac{2\pi}{q} (k-1) \right) + n\gamma \right] \end{cases} \quad (2)$$

Equation (2) gives a general torque expression for q-phase machine, which can be simplified into a standard form by inserting the value for q. The expression of Equation (2) can be simplified for three phase motor as

$$T_{em} = \frac{3\pi p D L_{stk}}{4} \sum_{n=1}^{\infty} \sum_{m=1}^{\infty} I_m B_n Z_n \cdot \cos(n \pm m | \omega t + n\gamma) \quad (3)$$

$$\begin{aligned} |n \pm m| &= 6c, \quad c=0,1,2,3,.. \\ m, n &= 1,5,7,11 \dots \end{aligned}$$

TORQUE RIPPLE MINIMISATION

Analysis of the above section gives torque harmonics T as a function of harmonics of flux density B, winding distribution Z and feed current I. Therefore, it is potentially possible to design a brushless DC motor for zero torque harmonics by suitable choice of B, Z and I. An interesting condition for three-phase motor, which is analyzed here, consists of considering I as a quasi-square then for given winding distribution and finding what B is needed to eliminate torque harmonics.

The interaction of fundamental current harmonic with 5th and 7th induced EMF harmonics produces 6th torque harmonic. Similarly, the interaction of fundamental induced EMF harmonic with 5th and 7th current harmonics produces 6th torque harmonic. The total 6th torque harmonic component is the algebraic sum of the interactions of m^{th} current harmonic with n^{th} induced EMF harmonic for $(m \pm n) = 6$.

Therefore, the total 6th harmonic component of torque can also be expressed as

$$T_6 = \frac{3}{2\omega_m} [E_1 I_5 + E_1 I_7 + E_5 I_1 + E_5 I_{11} + E_7 I_1 + E_7 I_{13} + E_{11} I_5 + E_{11} I_{17} + \dots]$$

or

$$T_6 = \frac{3}{2\omega_m} [E_1(I_5 + I_7) + E_5(I_1 + I_{11}) + E_7(I_1 + I_{13}) + E_{11}(I_5 + I_{17}) + \dots] \tag{4}$$

Similarly the higher order harmonic components of torque can be expressed as

$$T_{12} = \frac{3}{2\omega_m} [E_1(I_{11} + I_{13}) + E_5(I_7 + I_{17}) + E_7(I_5 + I_{19}) + E_{11}(I_1 + I_{23}) + \dots] \tag{5}$$

$$T_{18} = \frac{3}{2\omega_m} [E_1(I_{17} + I_{19}) + E_5(I_{13} + I_{23}) + E_7(I_{11} + I_{25}) + E_{11}(I_7 + I_{29}) + \dots] \tag{6}$$

The torque harmonics above the 18th, can also be expressed in the linear equation form as above. Evidently, the linear equations (4 to 6) can also be expressed in matrix form as

$$[T] = \frac{3}{2\omega_m} [I] \cdot [E] \tag{7}$$

where

$$[T] = [T_6 \quad T_{12} \quad T_{18} \quad T_{24} \quad \dots]^T \tag{8}$$

and

$$[E] = [E_1 \quad E_5 \quad E_7 \quad E_{11} \quad \dots]^T \tag{9}$$

$$[I] = \begin{bmatrix} (I_5 + I_7) & (I_1 + I_{11}) & (I_1 + I_{13}) & (I_5 + I_{17}) & \dots \\ (I_{11} + I_{13}) & (I_7 + I_{17}) & (I_5 + I_{19}) & (I_1 + I_{23}) & \dots \\ (I_{17} + I_{19}) & (I_{13} + I_{23}) & (I_{11} + I_{25}) & (I_7 + I_{29}) & \dots \\ (I_{23} + I_{25}) & (I_{19} + I_{29}) & (I_{17} + I_{31}) & (I_{13} + I_{35}) & \dots \\ \vdots & \vdots & \vdots & \vdots & \dots \\ \vdots & \vdots & \vdots & \vdots & \dots \end{bmatrix} \tag{10}$$

Equation system (7) can be used to calculate torque harmonics for a given design; more interesting is to work out design criteria for which torque harmonics are zero. To do this, torque harmonics can be replaced with zero, and induced EMF harmonics are calculated for known current harmonics by solving the following equation system (11):

$$\begin{bmatrix} (I_5 + I_7) & (I_1 + I_{11}) & (I_1 + I_{13}) & (I_5 + I_{17}) & \dots \\ (I_{11} + I_{13}) & (I_7 + I_{17}) & (I_5 + I_{19}) & (I_1 + I_{23}) & \dots \\ (I_{17} + I_{19}) & (I_{13} + I_{23}) & (I_{11} + I_{25}) & (I_7 + I_{29}) & \dots \\ (I_{23} + I_{25}) & (I_{19} + I_{29}) & (I_{17} + I_{31}) & (I_{13} + I_{35}) & \dots \\ \vdots & \vdots & \vdots & \vdots & \dots \\ \vdots & \vdots & \vdots & \vdots & \dots \end{bmatrix} \begin{bmatrix} E_1 \\ E_5 \\ E_7 \\ E_{11} \\ \vdots \\ \vdots \end{bmatrix} = \begin{bmatrix} 0 \\ 0 \\ 0 \\ 0 \\ \vdots \\ \vdots \end{bmatrix} \tag{11}$$

In practice, the above equation systems can be solved using computer methods and this was undertaken using the 'NAG' library routine 'F04ATF' [12]. This routine requires the set of real linear equations in the form '[A].[X]=[B]' where [A] and [B] are known input matrices and [X] is output solution matrix. Rearranging the above equation (11), gives;

$$\begin{bmatrix} (I_1 + I_{11}) & (I_1 + I_{13}) & (I_5 + I_{17}) & \dots \\ (I_7 + I_{17}) & (I_5 + I_{19}) & (I_1 + I_{23}) & \dots \\ (I_{13} + I_{23}) & (I_{11} + I_{25}) & (I_7 + I_{29}) & \dots \\ (I_{19} + I_{29}) & (I_{17} + I_{31}) & (I_{13} + I_{35}) & \dots \\ \vdots & \vdots & \vdots & \dots \\ \vdots & \vdots & \vdots & \dots \end{bmatrix} \begin{bmatrix} E_5 \\ E_7 \\ E_{11} \\ E_{13} \\ \vdots \\ \vdots \end{bmatrix} = \begin{bmatrix} -(I_5 + I_7)E_1 \\ -(I_{11} + I_{13})E_1 \\ -(I_{17} + I_{19})E_1 \\ -(I_{23} + I_{25})E_1 \\ \vdots \\ \vdots \end{bmatrix} \tag{12}$$

To calculate normalized induced EMF harmonics, the fundamental component 'E₁' in (12) can be replaced with '1.0', therefore;

$$\begin{bmatrix} (I_1 + I_{11}) & (I_1 + I_{13}) & (I_5 + I_{17}) & \dots \\ (I_7 + I_{17}) & (I_5 + I_{19}) & (I_1 + I_{23}) & \dots \\ (I_{13} + I_{23}) & (I_{11} + I_{25}) & (I_7 + I_{29}) & \dots \\ (I_{19} + I_{29}) & (I_{17} + I_{31}) & (I_{13} + I_{35}) & \dots \\ \vdots & \vdots & \vdots & \dots \\ \vdots & \vdots & \vdots & \dots \end{bmatrix} \begin{bmatrix} E_5 \\ E_7 \\ E_{11} \\ E_{13} \\ \vdots \\ \vdots \end{bmatrix} = \begin{bmatrix} -(I_5 + I_7) \\ -(I_{11} + I_{13}) \\ -(I_{17} + I_{19}) \\ -(I_{23} + I_{25}) \\ \vdots \\ \vdots \end{bmatrix} \tag{13}$$

For a quasi-square current, the current harmonics are known and the solution of (13) gives the normalized harmonics of induced EMF for torque ripple-free operation. Matrices A and B are calculated from known current harmonics and then 'NAG' subroutine is called to calculate unknown EMF harmonics for ripple-free torque operation. This routine calculates the accurate solution of a set of real simultaneous linear equations with a single right-hand side, using an 'LU' factorization with partial pivoting and iterative refinement until full machine accuracy [12].

The program was executed up to the order of 'A' matrix equal to 24. Above 24 the error flag IFAIL [12] returns with '2', which means iterative refinement failed to improve the solution. The induced EMF waveform plot, shown in Figure 1, follows a shape up to the order of 20. Above 20, the waveform is distorted due to truncation error. The solution of (13) gives induced EMF harmonics up to 61th. It can be seen from Figure 1, that the shape of the induced EMF waveform is close to six-step quasi-square wave as shown by dotted line. The rounding of the waveform at the edges is due to

limited size of the solution matrix. Theoretically, the size of the matrix should be infinite to get the exact waveform. The normalized induced EMF harmonics, obtained from the solution of (13) up to 19th, are listed in Table 1.

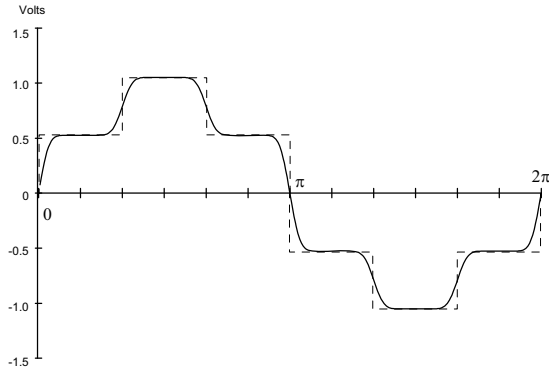


Figure 1: Construction of EMF plot from EMF harmonics calculated from 20 X20 matrix.

Table 1: Induced EMF harmonics calculated from 20X20 matrix.

n	E_n
1	1.0000
2	0.0000
3	0.0000
4	0.0000
5	0.1787
6	0.0000
7	-0.1140
8	0.0000
9	0.0000
10	0.0000
11	-0.0514
12	0.0000
13	0.0345
14	0.0000
15	0.0000
16	0.0000
17	0.0145
18	0.0000
19	-0.0089

Now, look at the design. The normalized flux density distribution harmonics can be synthesized from the knowledge of induced EMF harmonics and winding distribution harmonics as given in (14).

$$\begin{bmatrix} B_n \end{bmatrix} = \begin{bmatrix} E_n \\ Z_n \end{bmatrix} \tag{14}$$

Therefore, it is possible to design the flux density distribution harmonically from the induced EMF

harmonics calculated for constant torque operation. Next, few typical examples of winding designs are undertaken to calculate the harmonics and shape of B field for ripple-free torque operation. The synthesized harmonics of flux density, B are calculated from the truncated harmonics of E and Z up to 61th only.

One of the simplest stator winding is the full-pitch concentrated winding. For ideal concentrated full-pitch winding, the shape of induced EMF and flux density distribution is the same. However, it is impractical to get the shape of the flux density distribution as shown in Figure 1. As the triplen harmonics of flux density have been shown not to take part in the production of torque, the shape of the flux density distribution can be modified by the addition of triplen harmonics as illustrated in Figure 2.

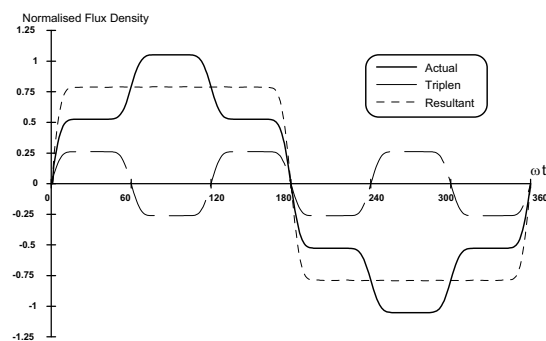


Figure 2: Synthesized flux density plot before and after addition of triplen harmonics.

The normalized flux plot synthesized from induced EMF harmonics is shown by the solid line in Figure 2. The flux plot constructed from added triplen harmonics is shown by the dashed line and the resultant flux plot obtained after the addition of triplen harmonics is shown by the dotted line. The flux density waveform after the addition of triplen can be obtained practically through iterative FEM analysis of the magnetic circuit as described in [13].

In 3-phase brushless DC machine, the winding should be distributed for an optimal design. However, the distribution of winding introduces torque pulsation. It is interesting to use the above design procedure for full pitch distributed winding. Table 2 shows the winding distribution harmonics and synthesized flux distribution harmonics obtained from (14), for concentrated, full-pitch winding and 10^o distributed, full-pitch winding. The harmonics for ideal rectangular B are also listed for comparison. It can be observed that the higher order harmonics are closer to ideal B , if the winding is distributed. The shape of flux density B , calculated from its harmonics is shown in Figure 3. It can be seen that the shape is nearly the same as for concentrated winding. It can be noted that the ripple-free torque operation is possible with practical winding and magnetic circuit designs.

Table 2: Winding harmonics and synthesized flux density distribution harmonics for full-pitch, concentrated winding.

n	Ideal		Full-pitch Concentrated Winding	
	B_n	Z_n	Z_n	B_n
1	1.0	1.0	1.0	1.0
3	0.3333	-1.0	-1.0	0
5	0.20	1.0	1.0	0.1787
7	0.1429	-1.0	-1.0	0.1140
9	0.1111	1.0	1.0	0
11	0.0909	-1.0	-1.0	0.0514
13	0.0769	1.0	1.0	0.0345
15	0.0667	-1.0	-1.0	0
17	0.0588	1.0	1.0	0.0145
19	0.0526	-1.0	-1.0	0.0089

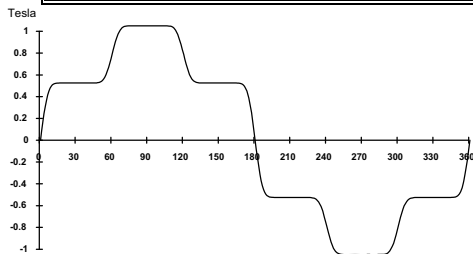


Figure 3: Flux density distribution plot for 10° distributed winding.

However, if the distribution of winding is increased above 10°, the synthesized shape of the flux density distribution changes from the one shown in Figure 3.

For example, the solution of (13) for slotless, 60° distributed winding, gives the shape of the flux density distribution as shown in Figure 4. The shape of flux density indicates that to get ripple-free torque operation for slotless, 60° distributed winding, the flux density should be concentrated. It is impractical to get concentrated flux density distribution of Figure 4 in the airgap of the machine. However, the mathematical solution obtained from the procedure is valid and interesting.

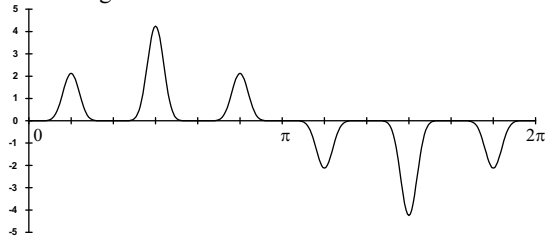


Figure 4: Flux-density distribution plot for full pitch, 60° distributed winding.

The flux density distribution is also synthesized for short pitch, concentrated type of winding. The

harmonics of flux density, calculated using (13), for a coil pitch of 175° are listed in Table 3.

The shape of flux density distribution in the airgap of the machine, for short-pitch concentrated type of winding, is calculated from the harmonics of Table 3 and shown in Figure 5. It can be seen that the synthesized shape of the flux density distribution for 175° pitched winding is nearly the same as for full-pitch winding.

Table 3: Winding harmonics and synthesized flux density distribution harmonics for short-pitch, concentrated winding.

n	Ideal		Short-pitch (175°) Concentrated Winding	
	B_n	Z_n	Z_n	B_n
1	1.0	1.0	1.0	1.0
3	0.3333	-0.9924	-0.9924	0
5	0.20	0.9772	0.9772	0.1829
7	0.1429	-0.9546	-0.9546	0.1194
9	0.1111	0.9248	0.9248	0
11	0.0909	-0.8879	-0.8879	0.0579
13	0.0769	0.8442	0.8442	0.0405
15	0.0667	-0.7941	-0.7941	0
17	0.0588	0.7380	0.7380	0.0056
19	0.0526	-0.6762	-0.6762	0.0035

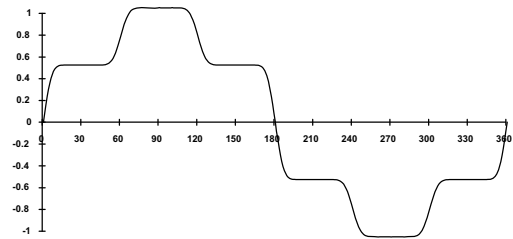


Figure 5: Flux density distribution plot for 175° pitched concentrated winding.

CONCLUSIONS

A new method of synthesizing flux density harmonics, with given winding distribution harmonics for zero torque harmonics, is described. A unique solution of induced EMF harmonics is obtained from this method and flux density harmonics and waveshapes are calculated for few winding designs. It is observed that triplen harmonics of flux density do not contribute to the torque production process. However, they can be used to improve the shape of the airgap flux density profile. Other sources of torque pulsation such as imperfect winding current and cogging are also discussed qualitatively.

The following conclusions can be drawn from this method of analysis:

- Table 1 gives a unique solution for the non-triplen induced EMF harmonics for ripple-free torque operation. This analysis suggests a unique solution of airgap flux density for any specific winding design.
- Triplen harmonics of flux density distribution do not effect the torque developed by the motor when driven by three-phase quasi-square current, but can be used to improve the shape of the airgap flux density.

REFERENCES

[1] Hendershot, J. R. and Miller, T. J. E., 'Design of brushless permanent magnet motors', Magna Physics Publishers and Clarendon Press Oxford 1994.

[2] Miller, T. J. E., 'Brushless permanent magnet and reluctance motor drives', Clarendon Press Oxford 1989.

[3] Le-Huy, H., Perret, R. and Feuillet, R., 'Minimisation of torque ripples in brushless DC motor drives', IEEE Transactions on Industry Applications, Vol. IA-22, No. 4, 1986.

[4] Nagase, H., Okuyama, T., Takahashi, J. and Saitoh, K., 'A method for suppressing torque ripple of an ac motor by current amplitude control', IEEE Transactions on Industrial Electronics, Vol. 36, No. 4, 1989, pp504-510.

[5] Ketteborough, J. G., Smith, I. R., Al-Hadithi, K. and Vadher, V. V., 'Current profiling for torque pulsation minimisation in brushless DC motor drives', Proc. EVS-11, Paper 8.09, 1992.

[6] Berendsen, C. S., Champenois, G. and Bolopion, A., 'Commutation strategies for brushless dc motors: influence on instant torque', IEEE Transactions on Power Electronics, Vol. 8, No. 2, 1993.

[7] Hanselman, D. C., 'Minimum torque ripple, maximum efficiency excitation of brushless permanent magnet motors', IEEE Transactions on Industrial Electronics, Vol. 41, No. 3, 1994.

[8] Bolton, H. R. and Ashen, R. A., 'Influence of motor design and feed current waveform on torque ripple in brushless dc drives', IEE Proc., Pt. B, Vol. 131, No. 3, 1984.

[9] Piriou, F., Razek, A. and Perret, R., 'Torque characteristics of brushless DC motors with imposed current waveform', IEEE Conference, IAS, 1986.

[10] Cho, K. -Y., Bae, J. -D., Chung, S. -K. and Youn, M. -J., 'Torque harmonics minimisation in permanent magnet synchronous motor with back EMF estimation', IEE Procs., Power App., Vol. 141, No. 6, November 1994.

[11] Izhar, T., and Evans, P. D., 'Permanent Magnet Multipole 6-phase Brushless DC motor for Automotive Application', 7th European conference on Power Electronics and Application, Trondheim, Norway 1997.

[12] 'FORTRAN NAG library manual Mark 16', Vol. 5, 1993.

[13] Izhar, T., 'Harmonic Presentation of Winding Distribution of Permanent Magnet Brushless DC Motor.' Journal of the Institution of Electrical and Electronics Engineers Pakistan VOL.NO.XXXVII, July 1998 to June 1999.